

Highly Advanced M&S System for Marine Accident Cause Investigation using FSI Analysis Technique

Sang-Gab Lee, Jae-Seok Lee, Hwan-Soo Lee

Korea Maritime & Ocean University, Marine Safety Technology

1 Abstract

Investigation of marine accident causes usually depends on the judgments of maritime experts, based on the statements of the concerned persons in the case where there is no navigation equipment, such as AIS and VDR. Scientific verification also has a limitation in the case of their conflicting statements. It is necessary to develop a highly advanced Modeling & Simulation (M&S) system for the scientific investigation of marine accident causes and for the systematic reproduction of accident damage procedure. To ensure an accurate and reasonable prediction of marine accident causes, full-scale ship collision, grounding, flooding and sinking simulations would be the best approach using hydrocode, such as LS-DYNA, with its Fluid-Structure Interaction (FSI) analysis technique and propulsion force for ship velocity. The objective of this paper is to present the findings from full-scale ship collision, grounding, flooding and sinking simulations of marine accidents, and to demonstrate the feasibility of the scientific investigation of marine accident causes using a highly advanced M&S system.

Keyword Words: *Highly Advanced Modeling & Simulation(M&S) System, Marine Accident Cause Investigation, Fluid-Structure Interaction(FSI) Analysis Technique, Full-Scale Ship Collision, Grounding, Flooding and Sinking Simulations, LS-DYNA code*

2 Introduction

It has been reported, from the statistics of marine accidents by the Korean Maritime Safety Tribunal (KMST) and the Lloyd's Maritime Information Services (LMIS), that collision, grounding and sinking accidents compose a majority of marine accidents, as shown in Fig. 1, bringing great loss of life and property, and hurting the ocean environment due to oil spills. Investigation of marine accident causes usually depends on the judgments of maritime experts, based on the statements of the concerned persons in the case where there is no navigation equipment, such as AIS and VDR. Scientific verification also has a limitation in the case of their conflicting statements. It is necessary to develop a highly advanced Modeling & Simulation (M&S) system for the scientific investigation of marine accident causes and for the systematic reproduction of what happens in marine accidents.

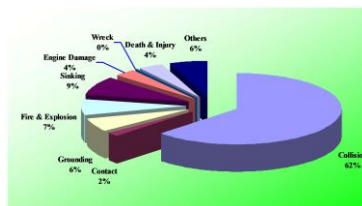


Fig. 1: Marine accidents according to type [1]

With the advent and ongoing advances in numerical simulation capabilities and its sophisticated tools, such as highly accurate dynamic nonlinear simulation hydrocode LS-DYNA [2], development of shock response analysis techniques has been actively carried out for the structural safety assessment with viable, less costly alternatives as well as more reliable aids to the tests and/or experiments. To ensure an accurate and reasonable prediction of shock response with relation to the fluid, such as explosion, sloshing, collision, grounding, flooding and sinking etc., full-scale simulations would be the best approach using hydrocode LS-DYNA with its Fluid-Structure Interaction (FSI) analysis technique. Several interaction effects in the water could be conceptualized in this highly advanced M&S system, such as floating, motion, wave making, squeezing pressure, bank effect and realistic ship velocity. Fracture criteria have to be also suitably applied to the structural damage considering strain rate effect, together with careful investigation of damage information.

FSI problems could be conveniently simulated by moving the mesh algorithm and overlap capability of the grid to structure mesh using the Multi-Material Arbitrary Lagrangian Eulerian (MMALE) formulation and the Euler–Lagrange coupling algorithm of LS-DYNA code, as shown in Fig. 2. This coupling algorithm would be more suitable for the FSI problems with very complicated deformable structure. Volume Of Fluid (VOF) method is adopted for solving a broad range of nonlinear free surface problems [3, 4]. Figure 3 depicts a schematic diagram of highly advanced M&S system for ship collision, grounding, flooding and sinking accidents, where external motion dynamics can be treated by the FSI analysis technique, internal damage mechanics, by considering reasonable fracture criteria with strain rate effect, and internal dynamics, by the internal fluid dynamics.

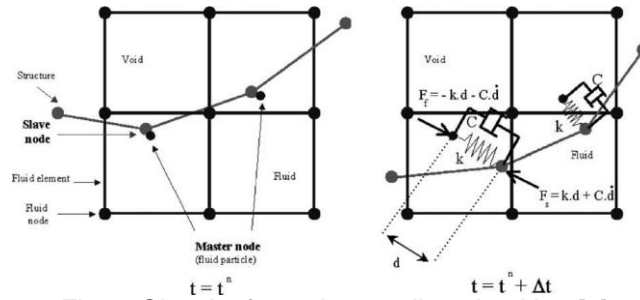


Fig. 2: Sketch of penalty coupling algorithm [3]

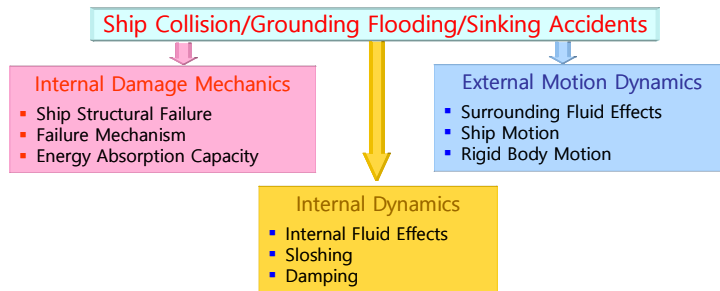
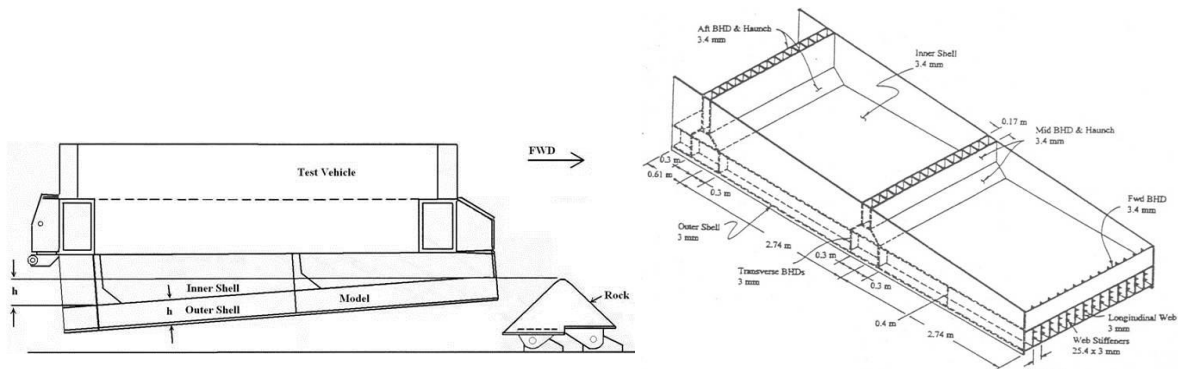


Fig. 3: Schematic diagram of highly advanced M&S system

In this study, typical full-scale ship collision, grounding, and flooding and sinking simulations were carried out to demonstrate the feasibility of the scientific investigation of marine accidents using highly advanced M&S system. This system was developed for the realization of rough sea state, such as breaking waves, and was applied to the investigation of flooding and sinking accident of the ship.

3 Internal Damage Mechanics

1:5 scale grounding test results of NSWC [5] are usually used for the verification of F.E. simulation capability and fracture criteria, as shown in Fig. 4. One of grounding test models, ADH/ PD328V, was simulated using rough and fine mesh models with failure strains from 0.20 to 0.35, as shown in Fig. 5, and material properties of ASTM 569, as shown in Table 1. It was found that failure strain 0.3 and 0.2 were suitable for the fine and rough meshes with ratio 12.5 and 25.0 of finite element size to thickness, respectively [6].



(a) grounding test setup

(b) double hull model ADH/PD328V

Fig. 4: Grounding test setup and model of NSWC [5]

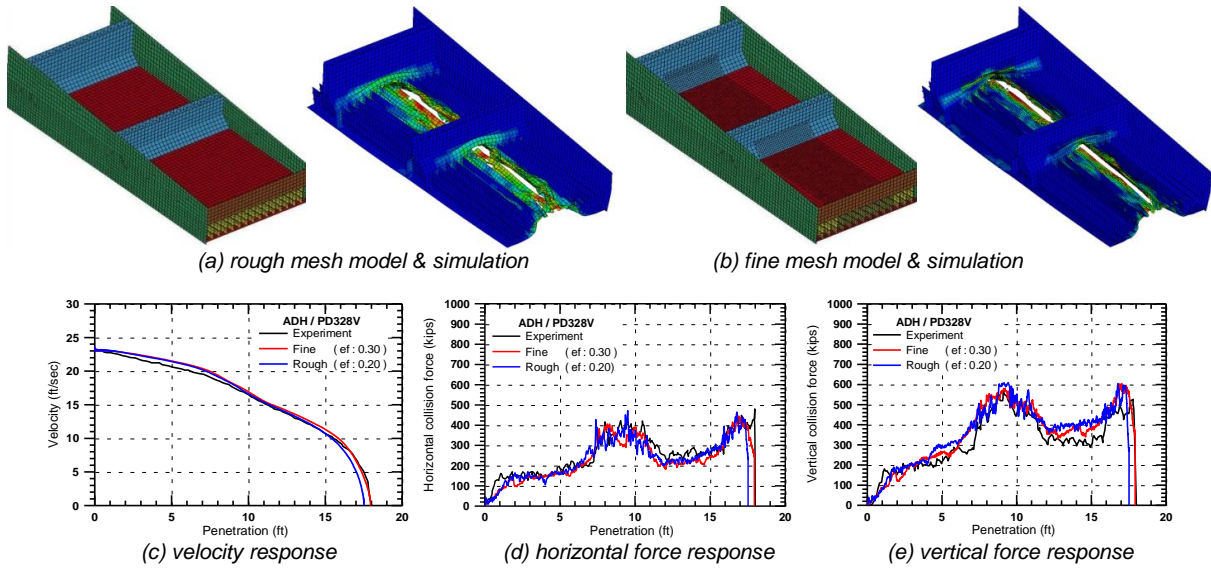


Fig. 5: Grounding test simulation of ADH/PD328V model

Table 1 Material properties of ASTM 569

Property	ASTM 569
Young's modulus	3.00×10 ⁷ ksi
Density	7.43×10 ⁻⁴ lbf-s ² /in
Poisson's ratio	0.30
Yield stress	41.00 ksi
Ultimate stress	50.00 ksi
Failure strain	0.20, 0.25, 0.30, 0.35
Dynamic yield stress constants	D=40.4 s ⁻¹ , q = 5

4 Highly Advanced M&S Simulation of Marine Accident

Full-scale ship collision, grounding, and flooding and sinking simulations were carried out to demonstrate the feasibility of the scientific investigation of marine accidents and reasonable structural safety assessment using highly advanced M&S system.

4.1 Investigation of collision accident of small fishing ship

Small fishing ship of gross tonnage 124 ton was known to be struck and sunk down to the bottom of river by the large cargo ship with at least gross tonnage 4,000 ton and over. The collision accident occurred during cross of the struck ship to the path of the striking ship. Figure 6 shows the damage configurations of the struck ship, where damage of number 2 might be due to the rope chain during salvage. F.E. mesh configurations of the striking and struck ships are shown in Fig. 7.



Fig. 6: Collision damage configuration of struck ship

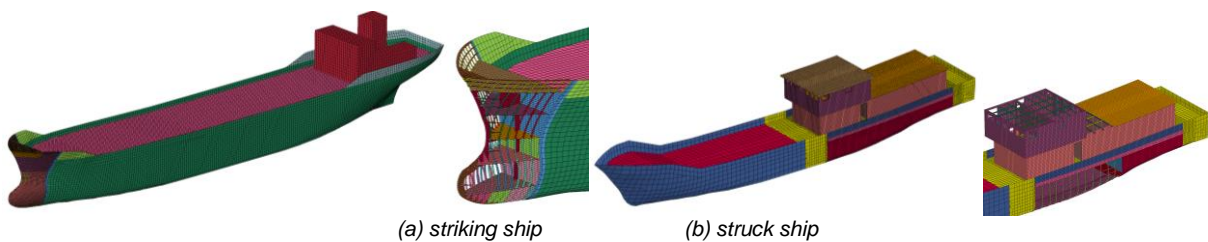
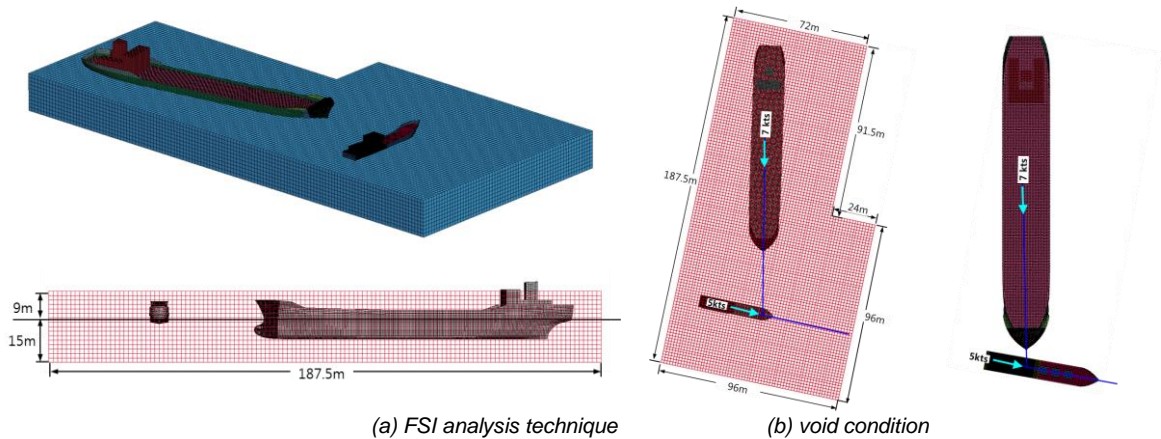


Fig. 7: F.E. mesh configurations of striking ship and struck one

Diverse scenarios were tried, such as collision attack angle, striking and struck ship velocity, for the investigation of collision and capsizing accident. In this study, among several scenarios, one collision simulation result, such as collision attack angle 70°, striking and struck ship velocities 7 and 5 knots, were treated, as shown in Fig. 8. For the comparison of simulation results using FSI analysis technique with those of conventional one, full-scale collision simulation was carried in void condition with the consideration of added mass, such as 1.1 times for the striking ship and 1.8 times for the struck one, where collision velocities were initial ones. In this study, mild and high tensile steels were used for the striking and struck ships, as shown in Table 2.



(a) FSI analysis technique (b) void condition
 Fig. 8: F.E. mesh configurations of full-scale collision simulation using FSI analysis technique & void condition

Table 2 Material properties of mild and high tensile steels

Property	Mild steel	High tensile steel
Young's modulus	206.0 GPa	206.0 GPa
Density	7,850 kg/m ³	7,850 kg/m ³
Yield stress	235.0 MPa	315.0 MPa
Ultimate stress	445.0 MPa	525.0 MPa
Failure strain	0.20, 0.25, 0.30	0.20, 0.25, 0.30
Dynamic yield stress constants	D=40.4 s ⁻¹ , q=5	D=24,804.6 s ⁻¹ , q=5

As expected, collision response behavior of full-scale collision simulation in void condition looks like unrealistic, as shown in Fig. 9. Very small damage, stress and plastic strain could be found in the rear top side of steering house, as shown in Fig. 10, and no damage, in the rear side shell in the simulation. Almost the same collision response behavior, damage, stress and plastic responses could be found with several scenarios in void condition. Exact investigation of collision accident could not be carried out in this simulation technique.

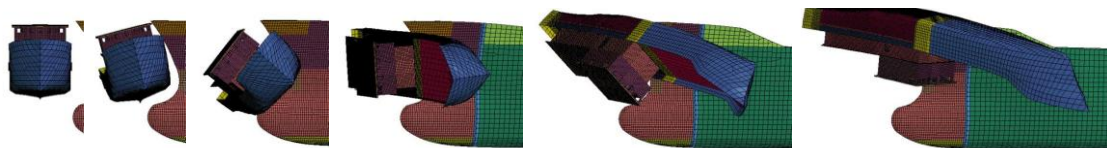
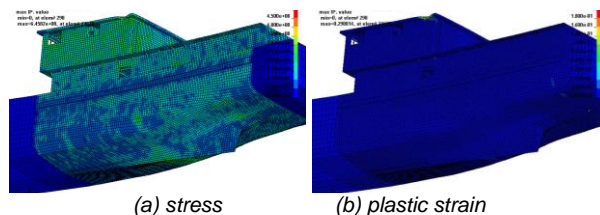


Fig. 9: Collision response behavior of full-scale collision simulation of small fishing ship in void condition



(a) stress (b) plastic strain
 Fig. 10: Stress and plastic strain response of struck ship in full-scale collision simulation in void condition

Figures 11~12 show overall and close views of collision response behaviors of full-scale collision simulation using FSI analysis technique, respectively. More accurate and realistic collision response behaviors could be found using FSI analysis technique. In this study, capsize and sinking problem was not considered because of insufficient time, however, these could be completed by the flooding simulation technique through the openings of small fishing ship. Stress and plastic strain responses are show in Fig. 13. These damage responses of small fishing ship could be found accurately to be the same as that of collision accident, as shown in Fig. 6.

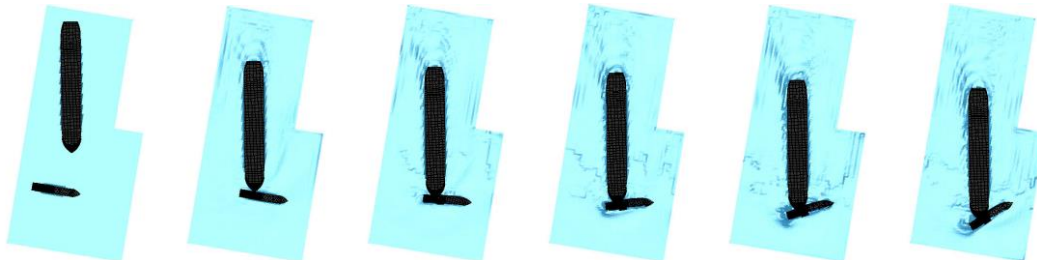


Fig. 11: Overall view of response behavior of full-scale collision simulation using FSI analysis technique

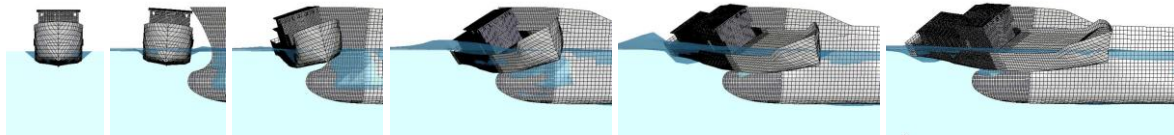


Fig. 12: Close view of response behavior of full-scale collision simulation using FSI analysis technique

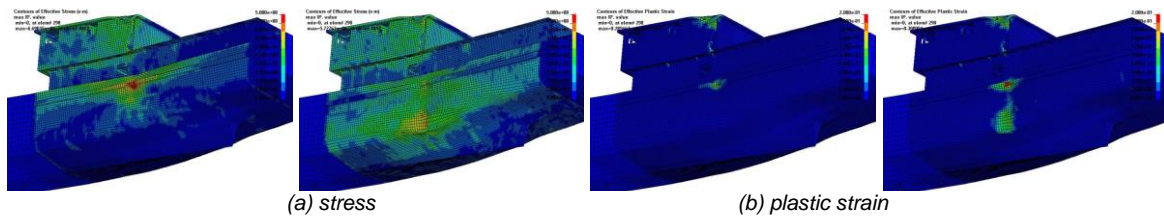


Fig. 13: Stress and plastic strain responses of struck ship in full-scale collision simulation using FSI analysis

4.2 Grounding safety assessment of specialized ship

Full-scale grounding simulation of the specialize ship with DWT 2,600 ton was performed for its structural safety assessment using FSI analysis technique and applying propulsion force to ship. Two grounding scenarios were considered for the rock position, such as center at the longitudinal line and 3.0m off the longitudinal one with full load condition. Figure 14 depicts the grounding scenarios, including fluid (seawater & air) model, where fluid model was decided for the enough space of ship motion and fluid boundary pressure reflection. Figure 15 shows the F.E. mesh configurations of the grounding ship and the rock, where bottom structure of the grounding one was modeled by the crushable deformable ones. In this study mild and high tensile steels were used for the specialized ship, as shown in Table 2.

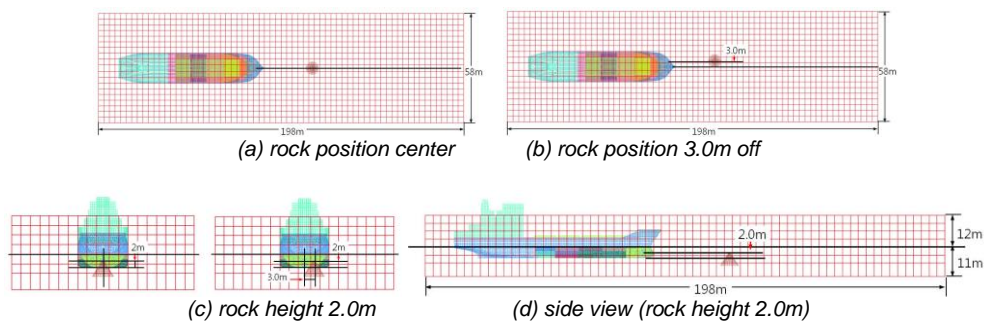


Fig. 14: Grounding scenario of specialized ship in full load condition

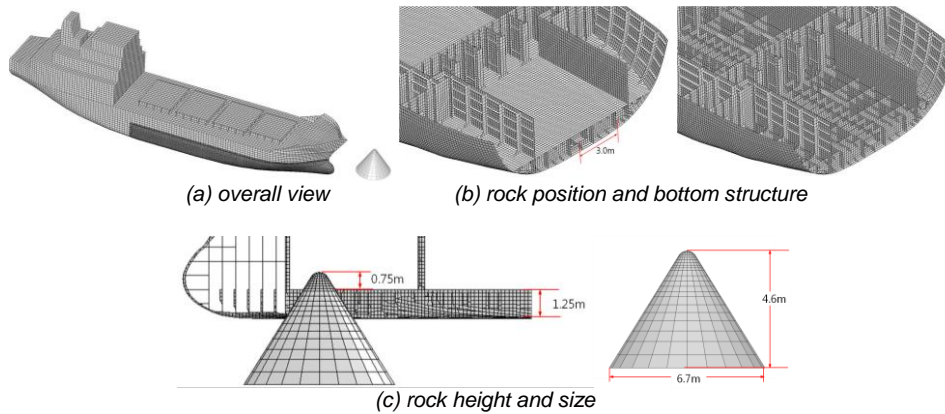


Fig. 15: F.E. configuration of grounding specialized ship and rock

Figures 18~19 illustrate the full-scale ship grounding response behaviors, with two rock positions, center and 3.0m off the longitudinal center line, at free motion and plane motion conditions in void, respectively, and Fig. 20, in sea water using FSI analysis technique.

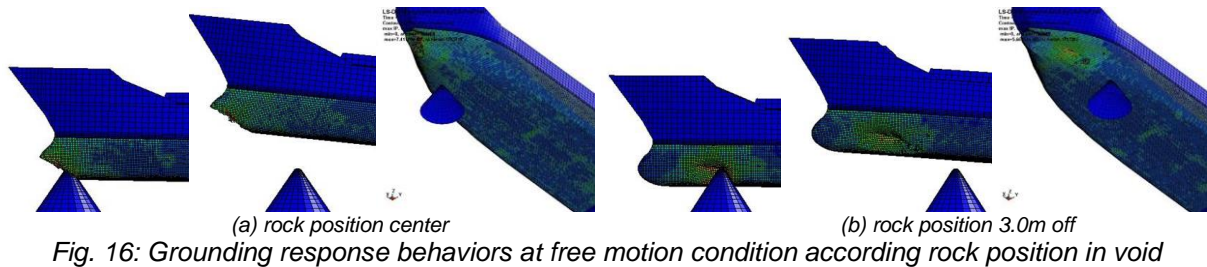


Fig. 16: Grounding response behaviors at free motion condition according rock position in void

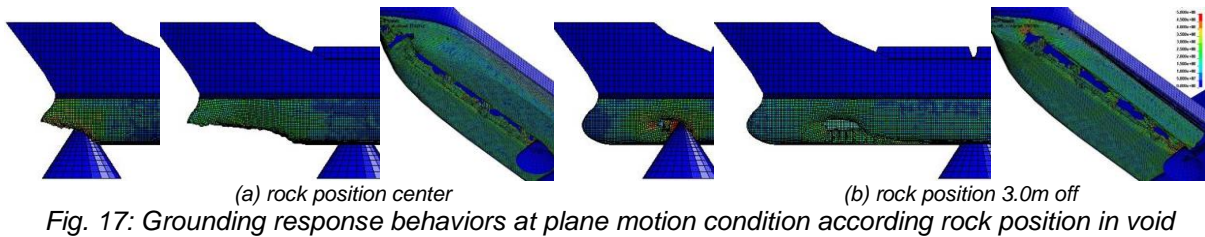


Fig. 17: Grounding response behaviors at plane motion condition according rock position in void

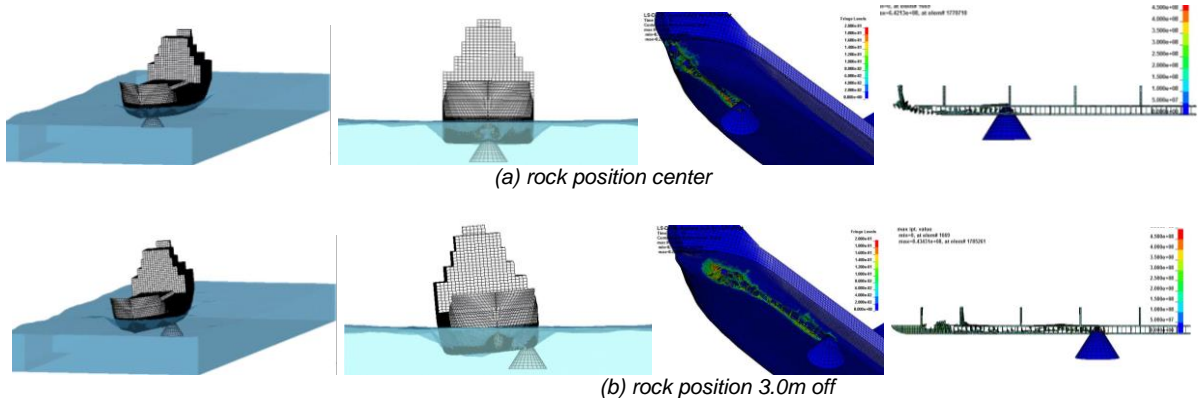


Fig. 18: Grounding response behaviors in free motion condition according to rock position in sea water

Contrary to the void condition, more realistic grounding response behaviors of the grounding ship, such as jumping and sway around the rock under the self-weight of grounding ship, could be found depending on the load condition and rock height and position using FSI analysis technique. There was no damage in the inner hull of the grounding ship in any grounding scenario in this study except very small stress concentration in the inner bottom hull in the case of full load condition with rock height 2.0m and center position. This might be due to the double bottom structure with good combination of longitudinal and transverse girder members.

4.3 Investigation of flooding and sinking accident of ship under breaking wave

The ship with displacement 400 ton under the quay outfitting was flooded and sunk down due to the tidal breaking wave under the bomb cyclone. In this study, full-scale ship flooding and sinking simulation was carried using FSI analysis technique for the investigation of flooding procedure through the openings and the estimation of the flooding duration. Table 3 shows the marine meteorological information of the ocean data (mooring) buoy at a distance around 40km away from quay, such as wind direction and gust speed, wave height and period, etc..

Table 3: Marine meteorological information of buoy

time	wind condition			atmospheric pressure (hPa)	humidity (%)	atmospheric temperature (°C)	water temperature (°C)	sea condition				
	direction	speed (m/s)	gust (m/s)					wave height(m)			period (sec)	direction
								max.	significant	average		
25. 04AM	WSW	13.8	17.3	101.3	83	14.8	16.6	4.8	4.1	2.0	8.0	S
25. 03AM	SW	15.9	20.1	1001.7	90	15.0	16.8	7.4	4.6	2.3	8.0	SSW
25. 02AM	S	17.2	23.0	999.5	81	18.8	16.9	6.2	3.8	1.9	8.0	WSW

Wave is usually classified as deep water, transitional water and shallow water waves according to the relationship of wave length (L) with water depth (h), as shown in Fig. 19(a). Three wave lengths are, $L=gT^2/2\pi$, $L=gT^2/2\pi \cdot \tanh(2\pi h/L)$, $L=\sqrt{gh}T$, respectively, where T is wave period. Wave length becomes shorter and wave height increase more with more sharp, the so-called breaking wave, as the deep water wave becomes to the shallow water one, where wave lengths of deep water and shallow water are 100.0m and 68.0m, respectively, in the case of wave period 8.0 sec, as shown in Table 3. Wave height of transition and shallow water wave, $H=L \cdot 0.17[1 - \exp\{-1.5\pi(h/L)(1+15\tan^{4/3}\beta)\}]$, is around 4.95m at the quay with water depth 7.3m [7]. Figure 19(b) illustrates the wave simulation response behavior depending on the water depth, from deep water depth 50.0m to shallow water depth 7.3m, where the shape, length and height of wave are represented relatively well.

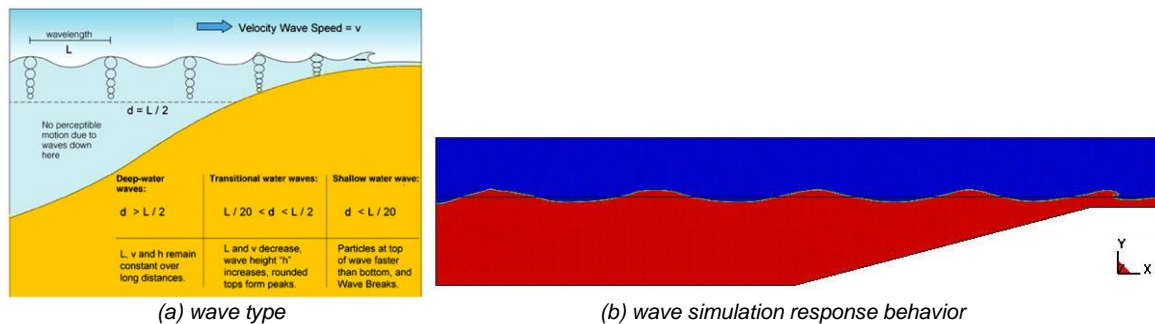


Fig. 19: Wave type and wave simulation response behavior according to water depth

As mentioned before, full-scale ship flooding and sinking simulation was carried out using FSI analysis technique. Figure 20(a) shows the F.E. mesh configurations of air and seawater MMALE model, and Fig. 20(b) ~ (c), the F.E. ones of seawater and ship including quay, fender, rope, etc.. Figure 20(b) also shows the piston plate for the realization of breaking wave. The ship is floating in the seawater at the draft 7.3m, also fastened by the 6 ropes and contacted by the air fenders and vertical dock fenders. The ship and air fenders could be floating, heaving, rolling and surging to the quay severely by the impact of breaking wave. The ship and air fenders are coupling to the air and seawater using CONSTRAINED_LAGRANGE_IN_SOLID option, and the ship, air fenders, vertical dock fenders and quay are contacted using CONTACT_AUTOMATIC_SURFACE_TO_SURFACE option.

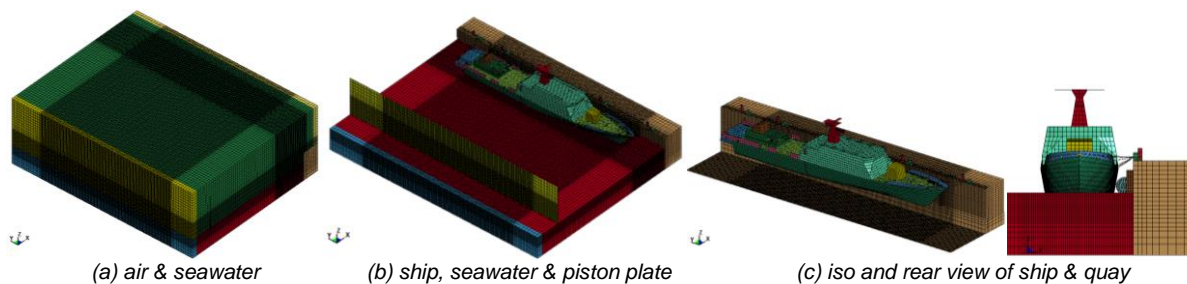


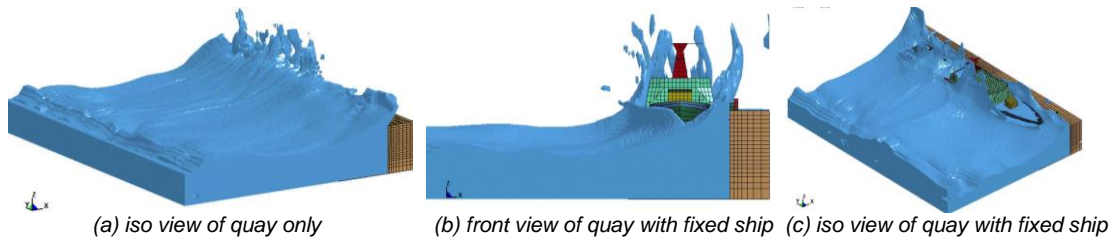
Fig. 20: F.E. mesh configuration of quay mooring model of ship including air and vertical dock fenders, rope using FSI analysis technique

There are many openings on the deck and superstructure, and in the watertight bulkheads, as shown in Fig. 21, where seawater could be flowed through the openings into the inboard of ship in the case of sweep of breaking wave over the deck and superstructure. After inflow of seawater, seawater could be propagated to the other compartments of the ship through the openings in the watertight bulkhead. These openings could not be closed for the outfitting process. Seawater was also coupled with the inside hull, bulkheads and engines, etc..



Fig. 21: F.E. mesh configuration of ship including openings on deck and superstructure, and watertight bulkheads

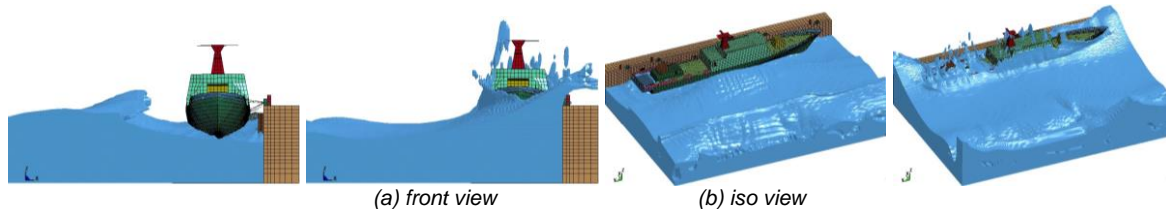
Figure 22 shows the breaking wave response behavior to the quay only and to the quay with fixed ship, using wave making piston plate, as shown in Fig. 20(b). For the reasonable motion of ship under the breaking wave, theoretical wave height 4.95m was reduced to 4.0m. The ship was trimmed by the stern with draft by bow 1.5m and draft by stern 2.6m. When tidal wave hit the ship directly and also the quay through the bottom of the ship, breaking wave swept the quarter deck and superstructure with trim by stern and seawater shot up between the ship and the quay, as shown in Fig. 22(b) ~ (c).



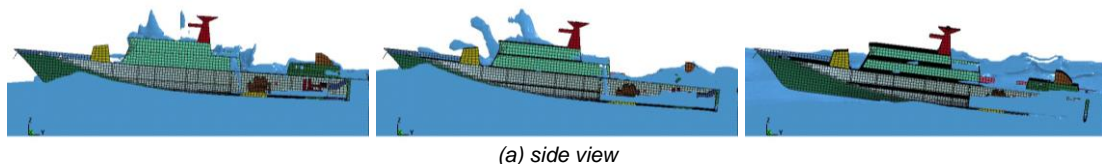
(a) iso view of quay only (b) front view of quay with fixed ship (c) iso view of quay with fixed ship
Fig. 22: Breaking wave simulation behavior to quay only and quay with fixed ship

Due to very large computational time in this full-scale ship flooding and sinking simulation using FSI analysis technique, this simulation was carried out by three steps; flooding through the opening of the quarter deck and superstructure in the engine compartments at the beginning step, flooding through the doors of the superstructure and through the openings of the deck, and propagation through the openings of watertight bulkheads to the accommodation compartments at the second step, and flooding through the doors of the superstructure, propagation in the superstructure and sinking down to the bottom at the last step.

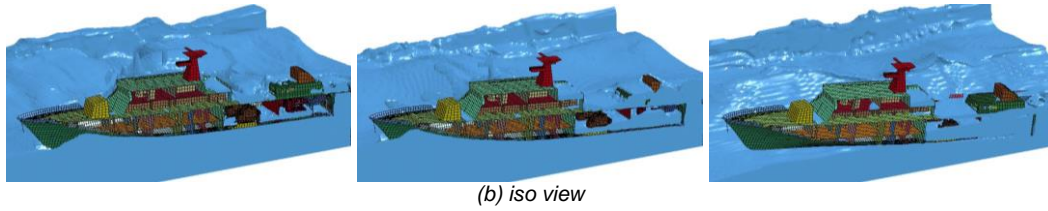
At the first step, the ship showed complicated motion of heaving, rolling and surging, and air fenders, heaving and surging, as shown in Fig. 23. Even though the breaking wave escaped through the gaps between the bulwarks, a lot of seawater was gathered on the deck surrounded by the bulwarks. It could be found that seawater flowed into the several openings of the deck and through the openings of the superstructure, and that the engine compartments became flooded gradually, as shown in Fig. 24.



(a) front view (b) iso view
Fig. 23: Breaking wave simulation behavior to mooring ship and quay

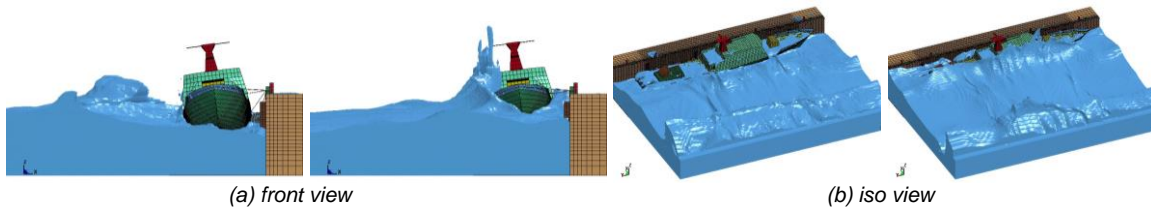


(a) side view

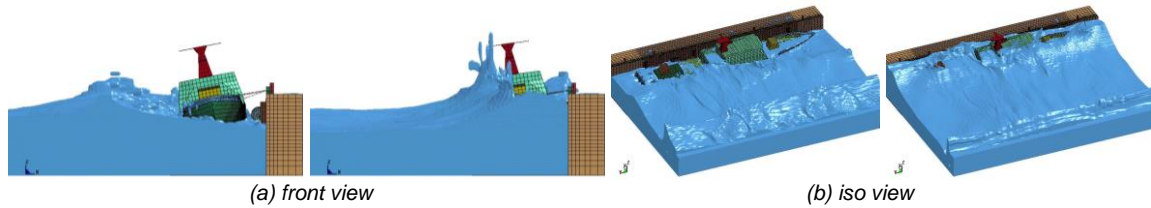


(b) iso view
 Fig. 24: Inflow of seawater through openings of deck and superstructure to engine compartments

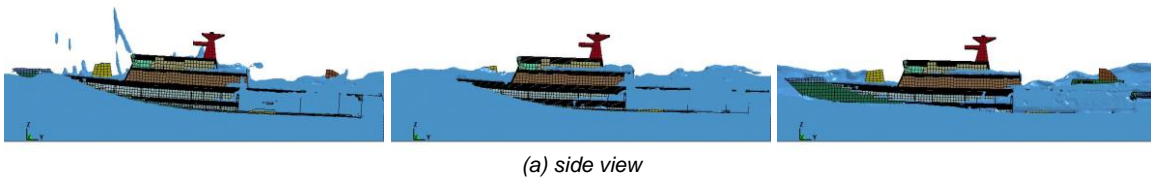
Figures 25~26 show the breaking wave response behaviors to the ship and quay and ship motion, depending on the breakage of the rear ropes at the second step. As the seawater flooded in the inboard of the ship, the rear of the ship trimmed by the stern more and moved more vertically and laterally, and the 5th, 6th and 4th ropes were cut off one by one with the increase of their tensile strengths, where the rear of the ship rolled out more to the starboard, as shown in Figs. 25~26. Seawater flowed through the doors of superstructure and through the openings of the deck, and propagated through the openings of the watertight bulkheads to the accommodation compartments, as shown in Fig. 27. Breaking wave also swept over the forecastle deck and seawater also flowed through the openings of the forecastle deck into the inboard compartments..



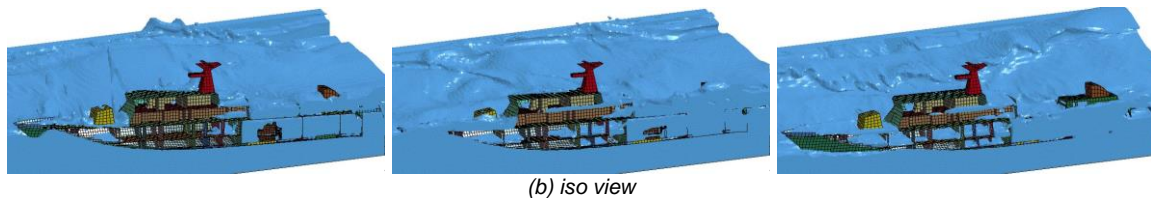
(a) front view (b) iso view
 Fig. 25: Breaking wave simulation behavior to mooring ship and quay with breakage of 5th & 6th ropes



(a) front view (b) iso view
 Fig. 26: Breaking wave simulation behavior to mooring ship and quay with breakage of 4th ~6th ropes



(a) side view



(b) iso view

Fig. 27: Inflow of seawater through openings of deck and superstructure and propagation to accommodation compartments

At the final step, Fig. 28 shows the breaking wave response behavior to the ship and quay, where the ship sank down more and rolled out more to the starboard. After seawater was flooded in the most compartments under the main deck, seawater flowed through the doors of the superstructure, as shown in Fig. 29, and the ship sank down more and the rear starboard bottom touched to the bottom. Through the full-scale ship flooding and sinking simulation using FSI analysis technique and realizing the rough sea condition, such as breaking wave, flooding and sink accident procedure could be investigated with high accuracy.

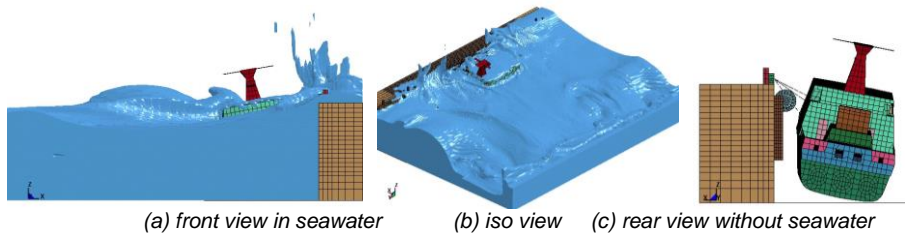


Fig. 28: Breaking wave simulation behavior to mooring ship and quay at final step

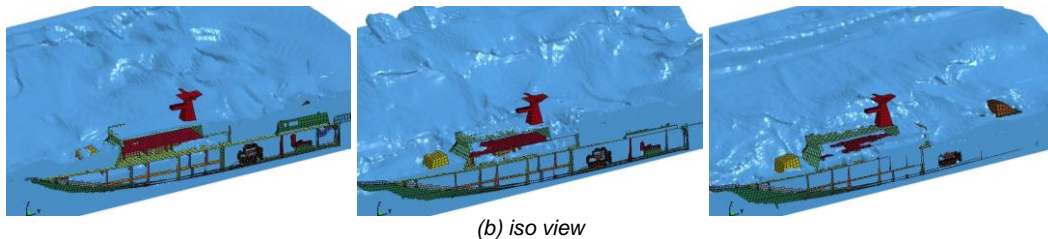
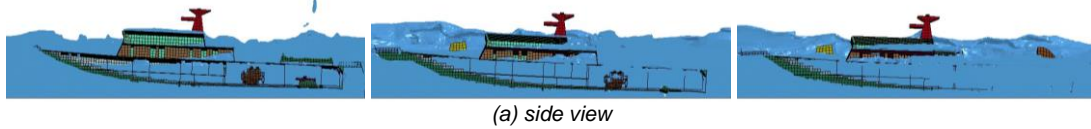


Fig. 29: Inflow of seawater through doors of superstructure and sink down to bottom

4.4 Investigation of collision accident between two ships

The first example is the investigation of collision accident between striking ship (cargo ship) and struck ship (pelagic fishing vessel) on the way of typhoon evasion. The struck ship sank down after its side bottom structure was torn away due to the bulbous bow's penetration of striking ship. Figure 30 shows the damage configurations and schematic damage drawings of the striking ship's forebody, such as the forecastle bulwark, the fashion plate and the bulbous bow, where the bulbous bow was torn away from starboard to port side with 1.2m size, and was also dented around bulbous bow with 1.5m radius quarter circle.

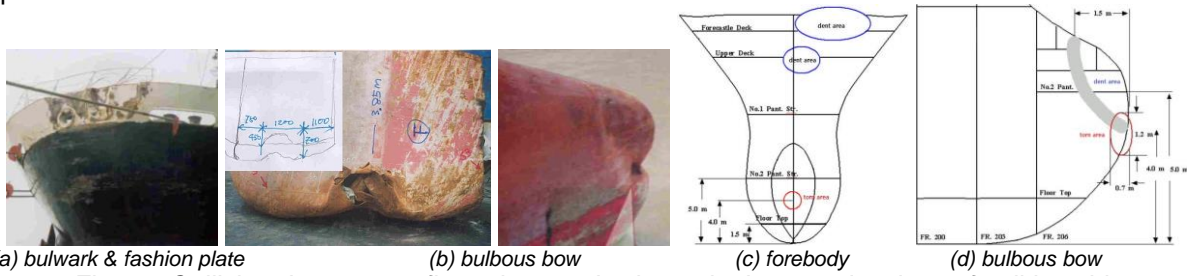


Fig. 30: Collision damage configurations and schematic damage drawings of striking ship

Figure 31 depicts the damage configurations of the struck ship's side superstructure, such as the derrick post and casing, and bottom side structure under free surface, such as side plate in the meal factory and bilge keel damage. From this damage configuration, it was found that the forecastle bulwark of the striking ship hit and pushed the derrick post of the struck one at 2.75m from the casing and that the fashion plate also pushed the casing during the collision.



Fig. 31: Collision damage configuration of struck ship's superstructure and bottom side structure

Schematic damage drawings were summarized from these damage configurations in Fig. 32. From the investigation of all collision damage information, a collision scenario between the two ships was sketched, as shown in Fig. 33(a). Fig. 33(b) depicts one collision scenario in a plan view among several ones, considering several attack angles, their speeds, and wind speeds and directions.

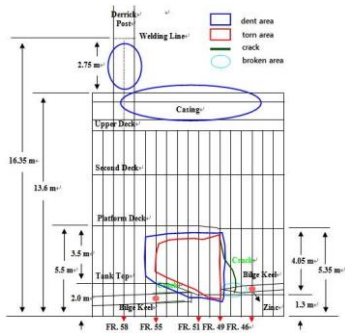


Fig. 32: Schematic damage drawings of struck ship

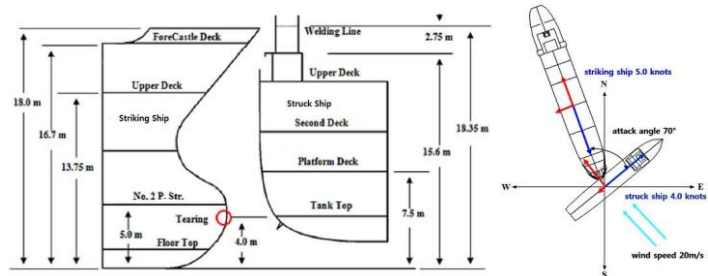


Fig. 33: Collision scenarios between two ships

Figure 34(a) shows the overall view of the F.E. mesh configuration for full-scale ship collision simulation using FSI analysis technique without air ALE part, and Figs. 34(b)–(c), the crushable fine ones of the striking and struck ships, respectively. Mild and high tensile steels were used for the ship structures, as shown in Table 2, where the strain rate dependent material of Cowper-Symonds was considered, failure strains 0.20, 0.25 and 0.30 according to the ratio of element size to thickness, and thickness was adjusted according to aging and corrosion. Figure 35 shows the overall and close views of full-scale ship collision behavior configurations, and Fig. 36, ship collision damage configurations. It was found that the motions of two ships are very important in full-scale ship collision simulation during collision between two ships, especially in the seawater.

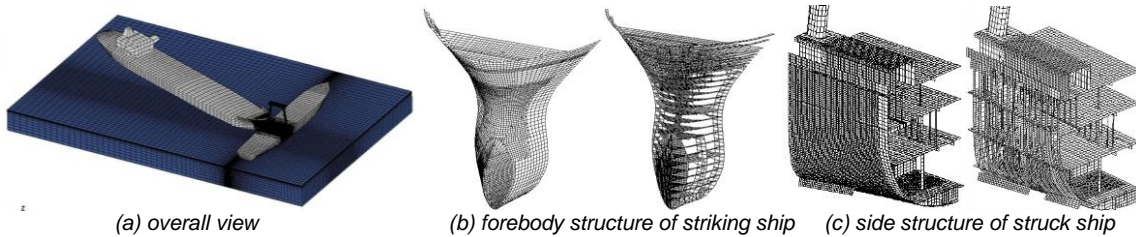


Fig. 34: F.E. mesh configurations of full-scale collision simulation using FSI analysis technique

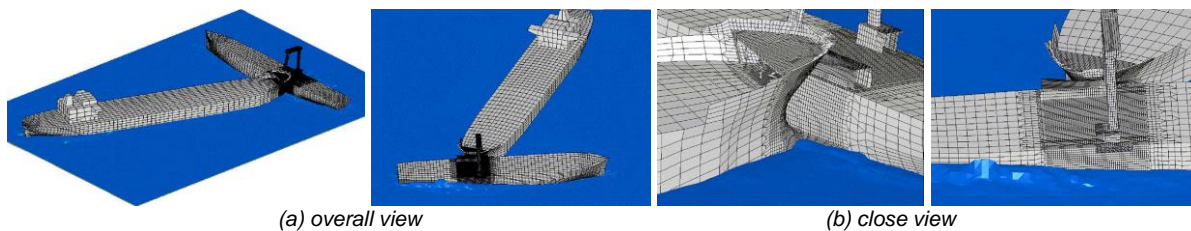


Fig. 35: Full-scale collision behavior configurations using FSI analysis technique

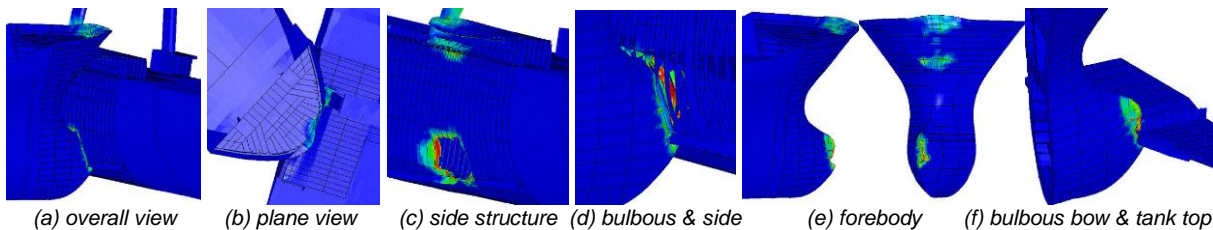


Fig. 36: Full-scale collision damage configurations using FSI analysis technique

The bottom side structure of the struck ship was penetrated by the bulbous bow of the striking one, and was torn away at around 4.0m in length (Fr. No. 56 ~ Fr. No. 50) and 4.0m in height (between the platform deck and the double bottom), even though the forecastle of the striking ship extends over the bulbous bow by 1.55m. This could have been possible due to the struck ship being turned around by

the collision of forecastle with the derrick post and the pushing down of the fashion plate to the casing in the seawater, and also due to the attack angle 70° and the speeds of the two ships and the wind, as shown in the collision scenario. The bulbous bow was dented by the side frame structure and the bulkhead of the struck ship, and torn away by the strong member, the tank top structure. This collision scenario and damage configuration could be confirmed by the judgment report of KMST (Korea Maritime Safety Tribunal), as shown in Fig. 37.

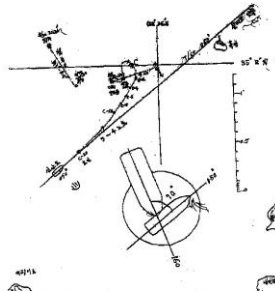


Fig. 37 Judgment report of KMST

5 Summary

Through full-scale ship collision, grounding, flooding and sinking simulations of marine accidents using FSI analysis technique, the usefulness of highly advanced M&S system could be reconfirmed for the scientific investigation of marine accidents and for the systematic reproduction of accidental damage procedure.

6 Literature

- [1] KMST: *KMST (Korea Maritime Safety Tribunal) Judgment Report*, 2002 ~ 2006.
- [2] LSTC: *LS-DYNA User's Manual, Version 971 R6*, Livermore Soft Technology Corp., USA, 2012..
- [3] Aquelet, N., Souli, M., and Olovsson, L.: "Euler-Lagrange coupling with damping effects: Application to slamming problems", *Computer Methods in Applied Mechanics and Engineering*, 195, 2006, pp. 110-132.
- [4] Souli, M., Ouahsine, A., and Lewin, L.: "ALE formulation for fluid-structure interaction problems", *Computer Methods in Applied Mechanics and Engineering*, 190, 2000, pp. 659-675.
- [5] Rodd, J., and Sikora, J.: "Double hull grounding experiments", *Proceedings of the 5th International Offshore and Polar Engineering Conference*, 1995, pp. 446-456.
- [6] Lee, S.G., Lee, J.S. and Yoon, Y.H.: "Fracture criterion on shock response analysis", *Proceedings of the Annual Autumn Conference, SNAK*, 2014, pp. 849-855.
- [7] Kim, D.S. and Lee, K.H.: *Coastal Engineering (Korean)*, Gumi Publisher, 2011.